electronics

MDPI

Communication

Quadratic Cascading in Quasi-Phase-Matching: An Alternative Route to Efficient Third-Harmonic Generation

Usman Sapaev [1,2] and Gaetano Assanto [3,*]

[1] Faculty of Electronics and Automation, Tashkent State Technical University, Universitetskaya Street 2, Almazar d/t, Tashkent 100095, Uzbekistan; u.sapaev@tdtu.uz
[2] Department of Physics, Electrical Engineering and Heat Engineering, The Tashkent Branch of the Russian Gubkin University, Durmon Yuli Street 34, Mirzo-Ulugbek d/t, Tashkent 100125, Uzbekistan
[3] NooEL—Nonlinear Optics and OptoElectronics Lab, Department IIEM, University "Roma Tre", 00146 Rome, Italy
* Correspondence: gaetano.assanto@uniroma3.it

Abstract: We report on the theoretical/numerical investigation of simultaneous second- and third-harmonic generation from a single wavelength input in quasi-phase-matched crystals. The presented technique consists of a quadratic crystal with two first-order quasi-phase-matched sections: one designed for quasi-phase-matching to second-harmonic generation and the other for quasi-phase-matching to third-harmonic generation via sum-frequency generation. We identify an optimal length ratio (optimal number of domains) for these sections in order to enhance the conversion to the third harmonic, achieving nearly complete energy transfer. The advantages of the method are demonstrated both numerically and analytically, with a specific example using periodically poled lithium niobate. Quadratic cascading with quasi-phase-matching proves to be an effective approach for achieving cubic-like effects with high conversion efficiencies.

Keywords: quadratic nonlinear optics; third-harmonic generation; second-harmonic generation; parametric cascading; quasi-phase-matching; ferroelectric crystals; parametric generation

check for updates

Citation: Sapaev, U.; Assanto, G. Quadratic Cascading in Quasi-Phase-Matching: An Alternative Route to Efficient Third-Harmonic Generation. *Electronics* **2024**, *13*, 4348. https://doi.org/10.3390/electronics13224348

Academic Editor: Nakkeeran Kaliyaperumal

Received: 2 September 2024
Revised: 16 September 2024
Accepted: 24 September 2024
Published: 6 November 2024

Copyright: © 2024 by the authors. Licensee MDPI, Basel, Switzerland. This article is an open access article distributed under the terms and conditions of the Creative Commons Attribution (CC BY) license (https://creativecommons.org/licenses/by/4.0/).

1. Introduction

Frequency conversion of laser light by means of nonlinear quadratic (i.e., $\chi^{(2)}$) processes holds significant value in several applications, while lasers can generate intense radiation at a single wavelength or a few wavelengths within a specific spectral interval, many applied as well as fundamental tasks require coherent radiation in spectral regions where laser light as-is is either unavailable or inefficiently produced. Since the very early days of lasers and nonlinear optics [1,2], the use of optical nonlinearity in $\chi^{(2)}$ media is known to offer solutions to this issue via three-photon parametric interactions, the primary benefit being the generation of coherent radiation with potentially high conversion efficiency [3–5]. Nevertheless, these quadratic media have limitations due to their finite transparency range, difficult momentum conservation, and damage threshold [3–5].

Although quadratically nonlinear dielectrics can be used for parametric processes involving three photons, homogeneous bulk media for cascaded parametric interactions such as third-harmonic generation (THG) via frequency-doubling (second-harmonic generation (SHG)) and sum-frequency generation (SFG) typically require sequential crystals, each satisfying momentum conservation (phase–velocity matching) for the chosen conversion process [6]. This usually involves side issues such as higher Fresnel losses, beam walk-off and diffraction, and orientation constraints due to birefringent phase-matching [4]. In contrast, quasi-phase-matched (e.g., periodically poled) crystals can operate under more favorable conditions [2], including fully degenerate polarization photon states, diffraction-less propagation in guided-wave configurations, mitigated control of crystal alignment, and/or temperature—a versatility stemming from the periodicity design [7]. Quasi-phase-matching

(QPM) relies on an average phase-matching over the crystal length by sign-alternating $\chi^{(2)}$ susceptibility domains: the periodic change in sign introduces a π phase change between successive contributions to the generated frequency component, effectively preventing the occurrence of destructive interference versus propagation, i.e., the well known Maker fringes [2,4]. QPM crystals can also exploit higher-order $\chi^{(2)}$ interactions and enable the simultaneous implementation of two (or more) coupled three-wave interactions by selecting the appropriate nonlinear domain size(s) [7,8].

When two quadratic processes are cascaded in noncentrosymmetric media with a $\chi^{(2)}$ susceptibility, they can exhibit an effective $\chi^{(3)}$ response under specific conditions, giving rise to the so-called "cascading nonlinearity". Cascaded parametric interactions in up- and down-conversion can yield efficient four-wave mixing effects such as self-phase modulation, producing a coherent intensity-dependent phase (or phase-front distortion) at the fundamental frequency ω, as normally ascribed to a Kerr-like nonlinear change in refractive index and supporting all-optical switching [9–14], spatial solitons [15–19] and gap solitons [20]. Moreover, as we shall analyze herein, it is possible to mimic a degenerate four-photon interaction such as THG by cascading SHG ($2\omega = \omega + \omega$) and SFG ($3\omega = 2\omega + \omega$). This allows for efficient THG from a single input wavelength, but is difficult to achieve in bulk crystals due to dispersion effects, as the three involved phase–velocities are largely unequal. The advantage of QPM crystals lies in the tailorability of the periodicity of the nonlinear grating for optimal performance, since adjustment of domain sizes can overcome the limitations of traditional $\chi^{(2)}$ crystals and enhance the efficiency and versatility of frequency conversion [21].

The simultaneous generation of second and third harmonics of a fundamental frequency input in a single crystal was addressed at the early stages of nonlinear optics in [22,23], where the authors discussed the dynamics of energy exchange between harmonics. A tutorial paper on the topic provides a detailed explanation of the physics behind frequency conversion [24].

In QPM-aided cascaded frequency conversion, various approaches have been discussed for third-harmonic generation from a single wavelength input. Among them, owing to the nonlinear trend of the dispersion relation in periodic crystals, one can simultaneously achieve quasi-phase-matching between ω and both 2ω and 3ω at the first [25] or higher-odd orders [26,27], as expressed by $\Delta k = k_2 - 2k_1 = k_3 - k_2 - k_1 = K$, where k_1, k_2, and k_3 are the wavenumbers of the fundamental, second, and third harmonics, respectively, and K is the wavenumber (1st-order) of the $\chi^{(2)}$ nonlinear grating itself. Interestingly, the condition above can be satisfied by optimizing the grating profile using random domain sizes, engineering the Fourier spectrum of the lattice with unequal domains [28–31]. Arranging domains with random lengths in quasi-phase-matched crystals, however, poses significant fabrication challenges to current technology [8,32]. An alternative approach is that of organizing the domains according to a Fibonacci series [33]. Moreover, designing the cross-sections of three-wave interactions has been demonstrated to support efficient third-harmonic generation [34]. Additional methods for efficient conversion of the fundamental to its third harmonic have been proposed, including those based on a specific ratio between the quadratic nonlinear coupling strenghts of the interacting harmonics [35,36] and on optimized input intensity levels at the first two harmonics [25]. These approaches, however, may be difficult to verify experimentally.

We have recently described an effective way to triple the input frequency in segmented QPM crystals [37], showing that there is an optimum ratio of segment lengths (or number of domains) that allows nearly complete energy conversion from the fundamental to its third harmonic. In this study, we discuss analytically how to design the best ratio of segment sizes for efficient THG in a $\chi^{(2)}$ sample with QPM gratings (see Figure 1). Despite that related configurations were tested for THG [38,39], the conditions for the most efficient third-harmonic generation in a crystal with QPM were not investigated.

In this Communication we report on a simple method for efficiently generating the third harmonic of a single frequency input in a quasi-phase-matched nonlinear crystal.

The crystal propagation length comprises two sections: the first ensures QPM to SHG and the second entails SFG to yield frequency tripling by adding first and second harmonics. Our numerical and analytical investigation reveals that a specific ratio between the QPM section lengths allows for essentially complete conversion of the fundamental to its third-harmonic. We believe that such an approach holds promises for a practical design of efficient frequency triplers in quadratic ferroelectric crystals.

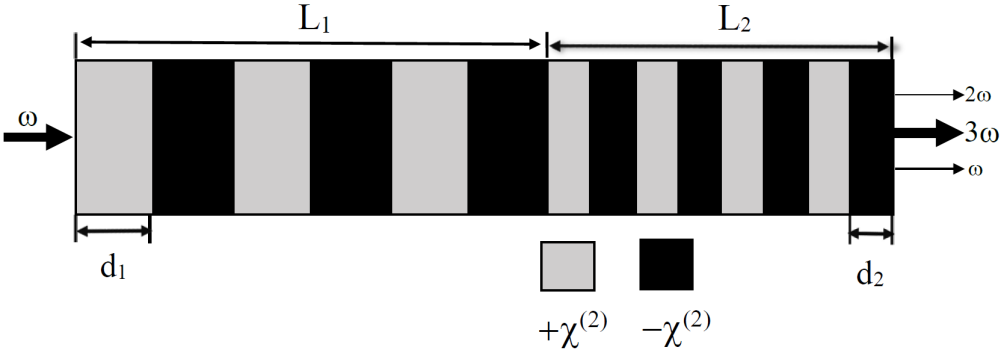


Figure 1. Illustration of a QPM lattice showcasing domain thicknesses d_1 and d_2, with alternating signs of the quadratic susceptibility $\chi^{(2)}$. Here, d_1 and d_2 represent the coherence lengths for the interactions $2\omega = \omega + \omega$ and $3\omega = 2\omega + \omega$, respectively. The sequential QPM sections L_1 and L_2 comply with momentum conservation (phase–velocity match) to second-harmonic and sum-frequency generations, respectively.

2. Method

As previously mentioned, the approach presented herein does not require a specific order of the QPM grating to generate the second and third harmonics of a fundamental. Nor is the simultaneous input of two (or three) frequencies at the input needed. The approach we focus on relies on a nonlinear susceptibility grating with two distinct sections L_1 and L_2 along the propagation path: the first section realizes the phase–velocity matching exclusively to the second harmonic, while the second implements QPM-mediated SFG to produce the third harmonic. Figure 1 illustrates the configuration under study. The QPM grating incorporates domain thicknesses d_1 and d_2 with alternating signs (but the same absolute value) of $\chi^{(2)}$. d_1 and d_2 are the coherence lengths of the interactions $2\omega = \omega + \omega$ (SHG) and $3\omega = 2\omega + \omega$ (SFG), respectively.

3. Model

In order to reduce design intricacies and underline the basic principle, we simply consider parametric interactions between CW plane waves co-propagating along z in the same polarization states. This allows employing first-order perturbation theory alongside the slowly varying phase and envelope approximation, both of which are easily extended to guided-wave interactions in channel waveguides through the adoption of coupled-mode-theory [4]. We assume, as usual, that Kleinmann symmetry holds in a purely dielectric crystal at all the wavelengths under consideration. Furthermore, we delve into Type 0 (ee-e) three-photon mixing involving triplets of extraordinarily polarized waves, with electric-fields parallel to z [28]. Naming A_j $(j = 1,2,3)$, the electric field amplitudes for the three waves at ω, 2ω, and 3ω, respectively, the coupled ODEs describing the cascaded interactions are:

$$\begin{aligned} \frac{dA_1(z)}{dz} &= -i\delta(z)A_1^*(z)A_2(z)e^{-i\Delta k_2 z} - i\delta(z)A_2^*(z)A_3(z)e^{-i\Delta k_3 z} \\ \frac{dA_2(z)}{dz} &= -2i\delta(z)A_1^*(z)A_3(z)e^{-i\Delta k_3 z} - i\delta(z)A_1^2(z)e^{i\Delta k_2 z} \\ \frac{dA_3(z)}{dz} &= -3i\delta(z)A_1(z)A_2(z)e^{i\Delta k_3 z} \end{aligned} \quad (1)$$

with $\delta(z) = \frac{4\pi\chi^{(2)}}{n(\lambda)\lambda} f(z)$ and the function $f(z)$ representing the spatially varying polarity. Here, k_j $(j = 1,2,3)$ are the wavenumbers at the involved frequencies ω, 2ω, and 3ω, respectively; $\Delta k_2 = k_2 - 2k_1$ is the phase mismatch for frequency doubling, and $\Delta k_3 = k_3 - k_2 - k_1$ is the phase mismatch for sum-frequency generation towards THG. In the system of ordinary differential Equations (1), we introduced the simplifying assumption $1/n(\lambda) \approx 1/n(\lambda/2) \approx 1/n(\lambda/3)$, where λ is the wavelength of the fundamental input, as well as the boundary conditions $A_1(z)|_{z=0} = A_0$, $A_2(z)|_{z=0} = 0$, and $A_3(z)|_{z=0} = 0$ (A_0 is the real amplitude of the electric field of the fundamental frequency wave at the input $z = 0$).

4. Analytical Solution

The system of ordinary differential Equations (1) admits an exact solution under specific conditions. To this extent, we first recast system (1) in a non-dimensional form, focusing on the second section of the sample where $\Delta k_3 = 0$. We consider only the real parts of the interacting harmonics and neglect energy exchange between the fundamental and the second harmonic in L_2, justified by $\Delta k_2 \neq 0$. System (1) then takes the dimensionless form:

$$\begin{aligned} \frac{da_1(x)}{dx} &= a_2(x)a_3(x) \\ \frac{da_2(x)}{dx} &= 2a_1(x)a_3(x) \\ \frac{da_3(x)}{dx} &= -3a_1(x)a_2(x) \end{aligned} \tag{2}$$

with a_1, a_2, and a_3 being the adimensionalized amplitudes at the three frequencies (i.e., $a_1(x) = A_1(x)/A_0$, $a_2(x) = A_2(x)/A_0$, and $a_3(x) = A_3(x)/A_0$), respectively, and the boundary conditions being $a_1(x)|_{x=L_1'} = a_{10}$ and $a_2(x)|_{x=L_1'} = a_{20}$.

Since a_{10} and a_{20} have to implement maximum third-harmonic generation at the output of the nonlinear optical sample, we can write:

$$\begin{aligned} a_1(x)|_{x=L_1'+L_2'} &\approx 0 \\ a_2(x)|_{L_1'+L_2'} &\approx 0 \\ a_3(x)|_{x=L_1'+L_2'} &\approx 1, \end{aligned} \tag{3}$$

with

$$\begin{aligned} \gamma &= \frac{8\chi^{(2)}}{n(\lambda_1)\lambda_1} \\ l_{nel} &= 1/(A_0\gamma) \\ \sqrt{a_{10}^2 + a_{20}^2} &= 1 \\ x &= z/l_{nel} \\ L_1' &= L_1/l_{nel} \\ L_2' &= L_2/l_{nel}. \end{aligned} \tag{4}$$

We can easily derive the relationship between the two boundary values a_{10} and a_{20} from the first and second equations of (2) as:

$$\frac{1}{a_2(x)}\frac{da_1(x)}{dx} = \frac{1}{2a_1(x)}\frac{da_2(x)}{dx}. \tag{5}$$

Then, from Equation (5) above, we get:

$$da_1^2(x) = \frac{1}{2}da_2^2(x). \tag{6}$$

Integrating the latter from $x = L_1'$ to $x = L_1' + L_2'$ and taking into account that $a_1(x)|_{x=L_1'+L_2'} \approx 0$ and $a_2(x)|_{x=L_1'+L_2'} \approx 0$, we obtain $a_{10} = a_{20}/\sqrt{2}$.

Since $\sqrt{a_{10}^2 + a_{20}^2} = 1$, we can solve for a_{10} and a_{20} and obtain $a_{20} = \sqrt{2/3}$ and $a_{10} = \sqrt{1/3}$. Hence, if the fundamental and second-harmonic waves satisfy these amplitude relationships at the end of section L_1, there will be complete conversion of all input (fundamental) energy to 3ω at the output of the sample, i.e., complete THG with full depletion of the fundamental.

To determine L_1' for which $a_1(x)|_{x=L_1'} = 1/\sqrt{3}$ and $a_2(x)|_{x=L_1'} = \sqrt{2/3}$, with $a_1(x)|_{x=0} = 1$ in the first segment of the QPM crystal, we can make use of the known exact solution for frequency doubling in phase-matching [2]. Thus, setting $a_{10} = 1/\sqrt{3} = \mathrm{sech}(L_1')$ (alternatively, $a_{20} = \sqrt{2/3} = \tanh(L_1')$), yields $L_1' = \ln(\sqrt{3} + \sqrt{2})$ (incidentally, employing the exact solution to the second harmonic leads to an identical result). Therefore, the number of domains in the first segment is

$$N_1 \approx \frac{\ln(\sqrt{3} + \sqrt{2})}{d_1} l_{nel}, \tag{7}$$

as we will validate in the following with numerical experiments.

The calculation of N_2 requires some further assumptions. The first consideration is that the boundary condition for the third harmonic at the end of the quasi-phase-matching crystal cannot be set to unity because there are always a few photons downconverted to the fundamental and second harmonics. Thereby, we can choose for the THG conversion efficiency b a number slightly less than 1 ($b * 1 - \epsilon$, with $\epsilon = (1)$). Secondly, we need to assume an intuitive function for the third-harmonic amplitude in the second segment. To this aim, we set $a_3(x) = \tanh(x)$ based on the trend of numerical computation, similar to the growth of the second-harmonic amplitude in the first segment.

We set the boundary condition $a_3(x)|_{x=L_1'} = 0$ and $a_3(x - L')|_{x=L_1'+L_2'} \approx b$, taking $b = 0.99$. Therefore, for $b = \tanh(L_2')$, we have $L_2 \approx 1.5$. Consequently, $N_2 \approx 1.5/d_2'$. In an actual design:

$$N_2 \approx \frac{1.5}{d_2} l_{nel} \tag{8}$$

We will demonstrate below that the values N_1 and N_2, given by expressions (7) and (8), respectively, provide the resonant conditions enabling the maximum conversion to the third harmonic in such a nonlinear optical sample.

5. Results and Discussion

We first examine the dynamics of three harmonics mutually coupled in an ideal, dimensionless nonlinear scenario with no losses. To this end, in Equation (1), we assume $|\delta(z)| = 1$, $d_1 = 0.01$, $d_2 = 0.003$, and $\gamma = 1$. For the boundary conditions, we set $A_1(z)|_{z=0} = 1$, $A_2(z)|_{z=0} = 0$, and $A_3(z)|_{z=0} = 0$. Using Equation (7), we find $N_1 \approx 180$ and, from Equation (8), $N_2 \approx 1570$, resulting in a total number of domains of 1750.

Numerical results are presented in Figure 2 for three cases: (i) when $L_1/L_2 = 1$, (ii) $N_1/N_2 = 1$, and (III) using the optimum conditions derived above. The blue-dashed line illustrates the outcome for the specified configuration with $N_1 = 180$ and $N_2 = 1570$. The solid-red and dotted-green lines show the cases with $L_1/L_2 = 1$ and $N_1/N_2 = 1$, respectively. It is apparent that the optimum design stemming from the analytical approach above allows achieving an essentially complete conversion to the third harmonic frequency.

We then examine a similar scenario under realistic conditions. To this extent, we select a periodically poled z-cut lithium niobate (LN) crystal. The linear and nonlinear optical properties of LN are extensively documented in the literature [40]. In such a noncentrosymmetric material, quadratic interactions can exploit the maximum second-order nonlinear susceptibility available for copolarized extraordinary waves in a Type 0 interaction. Specifically, the effective nonlinearity is $d_{eff} = d_{33} = \chi^{(2)}/2 \approx 26$ pm/V [28,40]. Such a large nonlinear coefficient facilitates efficient frequency conversion, making lithium niobate a suitable choice for parametric generation.

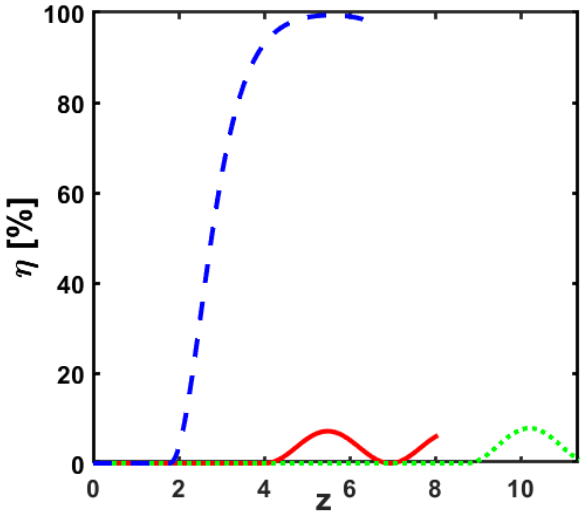


Figure 2. Calculated dynamics of energy conversion of the input fundamental to the triple frequency in a dimensionless sample with $|\delta(z)| = 1$, $d_1 = 0.01$, $d_2 = 0.003$, and $\gamma = 1$. The solid-red, dotted-green and dashed-blue lines correspond to (i) $L_1/L_2 = 1$, (ii) $N_1/N_2 = 1$, and (iii) $N_1 = 180$ and $N_2 = 1570$, respectively.

We calculate the energy exchange among the three harmonics versus propagation z in a ∼5 mm long periodically poled lithium niobate (PP-LN) crystal. The sample consists of two sections: the first is quasi-phase-matched to SHG and the second is QPM-ed to the SFG based on the fundamental and second-harmonic waves. The input wavelength is set to $\lambda = 1.52$ µm with an intensity of 0.1 GW/cm^2. Under these conditions, the domain lengths are $d_1 \approx 9.07$ µm for SHG and $d_2 \approx 3.23$ µm in the THG Section [28]. These values are crucial for optimizing the conversion efficiency through the cascaded interactions.

Figure 3 shows the conversion efficiency η in THG versus sample length, assuming the optimal values $N_1 = 133$ and $N_2 = 978$ in the two QPM sections, as determined from Equations (7) and (8). This choice of domain numbers nearly achieves complete energy conversion of the fundamental to the third-harmonic wave, as graphed by the blue-dashed line. The energy transfer from ω and 2ω to 3ω is well visible, with η approaching 100%. Noteworthy other factors, such as higher-order nonlinearities and dispersion effects, can be neglected in this case due to the relatively short nonlinear optical sample.

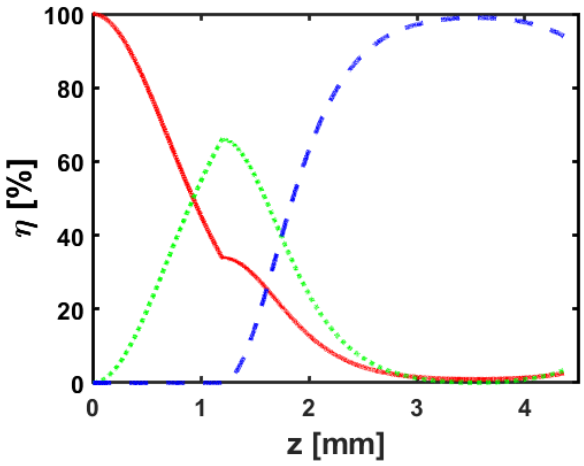


Figure 3. Results of a numerical experiment in a realistic PP-LN sample approximately 5 mm in length. The input wavelength is $\lambda = 1.52$ µm with an intensity of 0.1 GW/cm^2. The total domain number was $N = 1111$ ($N_1 = 133$ and $N_2 = 978$). The blue-dashed, green-dotted, and red-solid lines represent the third, second, and fundamental harmonics, respectively. The change in slope in the red and green curves corresponds to the variation in QPM periodicity between the sections.

We further investigated THG versus input intensity values while keeping N_1 and N_2 fixed. Typical results are displayed in Figure 4 for the same PP-LN sample as above. The solid lines in red, green, and black (labels 1, 2, and 3, respectively) are the THG efficiencies calculated for three different input intensities at the fundamental frequency wave: 0.11 GW/cm^2, 0.5 GW/cm^2, and 1.5 GW/cm^2, respectively. The blue dashes refer to the input intensity for which the optimum conditions were derived above (Figure 2). Clearly, the best conversion is achieved at an intensity of 0.1 GW/cm^2. However, as the input intensity increases, the maximum efficiency reduces. While this suggests that optimum conditions apply at a specific intensity, minor deviations result in satisfactory performances.

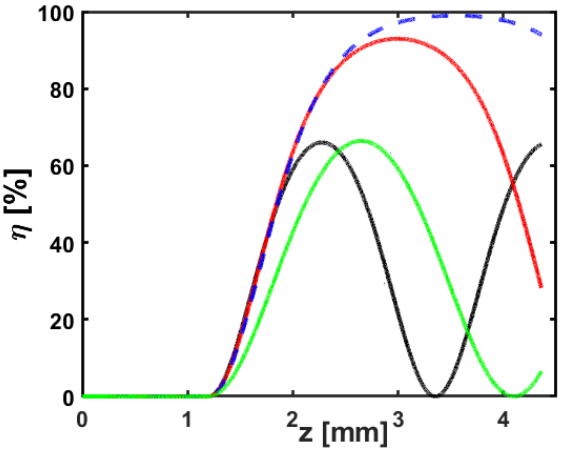


Figure 4. Numerical experiments in a realistic periodically poled lithium niobate sample approximately 5 mm long. The wavelength is λ = 1.52 μm with input intensities 0.1 (blue dashes), 0.11 (red solid line), 0.5 (green solid line), and 1.5 (black solid line) GW/cm^2, respectively. The total number of domains was set to N = 1111, with N_1 = 133 and N_2 = 978.

Finally, we studied the impact of the ratio N_1/N_2 on THG conversion efficiency in order to assess the validity of the analytical solution. The results of these simulations are presented in Figure 5, plotting THG efficiency versus $\alpha = N_1/N_2$ across a range of input intensities. The Figure clearly shows that the analytical method is rather accurate in providing the optimum ratio N_1/N_2 (with $\alpha \approx 1.36$). Furthermore, it is apparent that maximum THG can only be achieved in a narrow interval of α values. This analysis considered a realistic periodically poled LN crystal, with parameters as detailed in Figures 3 and 4.

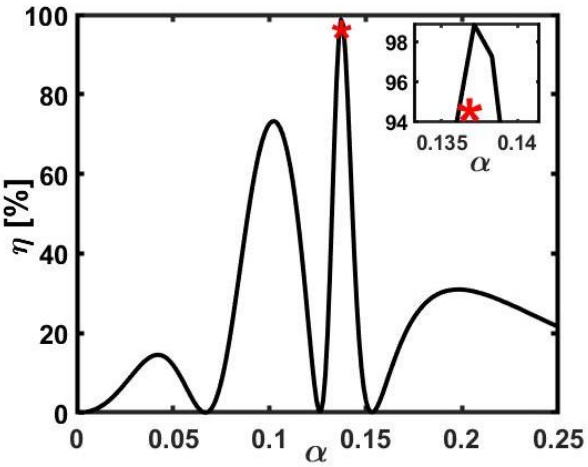


Figure 5. Results of numerical experiments in a realistic PP-LN sample, with $\lambda = 1.52\,\mu$m, 0.1 GW/cm^2, $N = 1111$, $d_1 \approx 9.07\,\mu$m, and $d_2 \approx 3.23\,\mu$m. Here, we graph the THG efficiency η versus $\alpha = N_1/N_2$ for a constant number of total domains N. The red star marks the analytically calculated value of $\alpha \approx 0.136$. The inset is a zoomed-in detail around this value.

6. Conclusions

In this Communication, we have presented a novel approach to model and simulate the simultaneous generation of the second and third harmonics of a single fundamental input wave in periodically engineered crystals. We analyzed noncentrosymmetric crystal samples designed/optimized for second-harmonic generation and for sum-frequency generation of the first two harmonics, yielding third-harmonic generation via quadratic cascading. The method and solutions allow for the best ratio of the section lengths to be estimated, ensuring the highest conversion efficiency from ω to 3ω in the plane-wave and CW limits over a finite propagation length and under realistic conditions.

The results, validated through numerical experiments, underscore the effectiveness of the approach. Notably, the use of periodically poled lithium niobate demonstrates significant potential for enhanced harmonic generation in frequency tripling. We also pinpointed the tolerances to input intensity and grating design.

We believe that our findings can contribute to designing highly efficient parametric optical processes to be implemented via quadratic cascading in periodically poled quadratic crystals.

Author Contributions: U.S.: Writing—original draft, Methodology, Investigation, Formal analysis, Conceptualization. G.A.: Writing—review and editing, Supervision, Conceptualization. All authors have read and agreed to the published version of the manuscript.

Funding: U.S. acknowledges partial financial support through the MUNIS Project grant REP-04032022-206, funded by the World Bank and the Republic of Uzbekistan.

Institutional Review Board Statement: Not applicable.

Informed Consent Statement: Not applicable.

Data Availability Statement: Data will be made available on request.

Conflicts of Interest: The authors declare no conflicts of interests.

References

1. Franken, P.A.; Hill, A.E.; Peters, C.W.; Weinreich, G. Generation of Optical Harmonics. *Phys. Rev. Lett.* **1961**, *7*, 118–120. [CrossRef]
2. Armstrong, J.A.; Bloembergen, N.; Ducuing, J.; Pershan, P.S. Interactions between Light Waves in a Nonlinear Dielectric. *Phys. Rev. Lett.* **1962**, *127*, 1918–1939. [CrossRef]
3. Boyd, R.W.; Gaeta, A.L.; Giese, E. Nonlinear optics. In *Springer Handbook of Atomic, Molecular, and Optical Physics*; Springer: Berlin/Heidelberg, Germany, 2008; pp. 1097–1110.
4. Stegeman, G.I.; Stegeman, R.A. *Nonlinear Optics: Phenomena, Materials and Devices*; John Wiley & Sons: Hoboken, NJ, USA, 2012.
5. Li, C. *Nonlinear Optics: Principles and Applications*; Springer: Berlin/Heidelberg, Germany, 2016.
6. Craxton, R.S. Theory of high efficiency third harmonic generation of high power Nd-glass laser radiation. *Opt. Commun.* **1980**, *34*, 474–478. [CrossRef]
7. Fejer, M.M.; Magel, G.A.; Jundt, D.H.; Byer, R.L. Quasi-phase-matched second harmonic generation: Tuning and tolerances. *IEEE J. Quantum Electron.* **1992**, *28*, 2631–2654. [CrossRef]
8. Hum, D.S.; Fejer, M.M. Quasi-phasematching. *Comptes Rendus Phys.* **2007**, *8*, 180–198. [CrossRef]
9. Stegeman, G.I.; Sheik-Bahae, M.; Van Stryland, E.; Assanto, G. Large nonlinear phase shifts in second-order nonlinear-optical processes. *Opt. Lett.* **1993**, *18*, 13–15. [CrossRef]
10. Assanto, G.; Stegeman, G.; Sheik-Bahae, M.; Van Stryland, E. All-optical switching devices based on large nonlinear phase shifts from second harmonic generation. *Appl. Phys. Lett.* **1993**, *62*, 1323–1325. [CrossRef]
11. Hagan, D.J.; Wang, Z.; Stegeman, G.; Van Stryland, E.W.; Sheik-Bahae, M.; Assanto, G. Phase-controlled transistor action by cascading of second-order nonlinearities in KTP. *Opt. Lett.* **1994**, *19*, 1305–1307. [CrossRef]
12. Assanto, G.; Stegeman, G.I.; Sheik-Bahae, M.; VanStryland, E. Coherent interactions for all-optical signal processing via quadratic nonlinearities. *IEEE J. Quantum Electron.* **1995**, *31*, 673–681. [CrossRef]
13. Stegeman, G.I.; Hagan, D.J.; Torner, L. $\chi^{(2)}$ cascading phenomena and their applications to all-optical signal processing, mode-locking, pulse compression and solitons. *Opt. Quantum Electron.* **1996**, *28*, 1691–1740. [CrossRef]
14. Assanto, G. Transistor action through nonlinear cascading in Type II interactions. *Opt. Lett.* **1995**, *20*, 1595–1597. [CrossRef]
15. Schiek, R.; Baek, Y.; Stegeman, G.; Sohler, W. One-dimensional quadratic walking solitons. *Opt. Lett.* **1999**, *24*, 83–85. [CrossRef]
16. Picciau, M.; Leo, G.; Assanto, G. Versatile bistable gate based on quadratic cascading in a Bragg periodic structure. *J. Opt. Soc. Am. B* **1996**, *13*, 661–670. [CrossRef]

17. Costantini, B.; De Angelis, C.; Barthelemy, A.; Laureti Palma, A.; Assanto, G. Polarization multiplexed $\chi^{(2)}$ solitary waves interactions. *Opt. Lett.* **1997**, *22*, 1376–1378. [CrossRef]
18. Leo, G.; Assanto, G.; Torruellas, W.E. Bidimensional spatial solitary waves in quadratically nonlinear bulk media. *J. Opt. Soc. Am. B* **1997**, *14*, 3134–3142 [CrossRef]
19. Gallo, K.; Pasquazi, A.; Stivala, S.; Assanto, G. Parametric Solitons in Two-Dimensional Lattices of Purely Nonlinear Origin. *Phys. Rev. Lett.* **2008**, *100*, 053901. [CrossRef]
20. Conti, C.; Trillo, S.; Assanto, G. Doubly Resonant Bragg Simultons via Second-Harmonic Generation. *Phys. Rev. Lett.* **1997**, *78*, 2341–2344. [CrossRef]
21. Chen, B.Q.; Zhang, C.; Hu, C.Y.; Liu, R.J.; Li, Z.Y. High-efficiency broadband high-harmonic generation from a single quasi-phase-matching nonlinear crystal. *Phys. Rev. Lett.* **2015**, *115*, 083902. [CrossRef]
22. Akhmanov, S.A.; Dmitriev, V.G.; Modenov, V.P. Towards the theory of frequency multiplication in nonlinear dispersive lines. *Radiotech. Electron.* **1964**, *9*, 13–20.
23. Akhmanov, S.A.; Khokhlov, R.V. *Problems of Nonlinear Optics: Electromagnetic Waves in Nonlinear Dispersive Media*; Gordon and Breach: Moscow, Russia, 1972.
24. Hareli, L.; Shoulga, G.; Bahabad, A. Phase matching and quasi-phase matching of high-order harmonic generation—A tutorial. *J. Phys. B At. Mol. Opt. Phys.* **2020**, *53*, 233001. [CrossRef]
25. Sapaev, U.K.; Kulagin, I.A.; Satlikov, N. Kh.; Usmanov, T. Optimization of third harmonic generation for two coupled three-frequency interactions of waves with multiple frequencies in periodic crystals. *Opt. Spectr.* **2006**, *101*, 983–985. [CrossRef]
26. Aleksandrovski, A.L.; Chirkin, A.S.; Volkov, V.V. Realization of quasi-phase-matched parametric interactions of waves of multiple frequencies with simultaneous frequency doubling. *J. Russ. Las. Res.* **1997**, *18*, 101–106. [CrossRef]
27. Pfister, O.; Wells, J.S.; Hollberg, L.; Zink, L.; Van Baak, D.A.; Levenson, M.D.; Bosenberg, W.R. Continuous-wave frequency tripling and quadrupling by simultaneous three-wave mixings in periodically poled crystals: Application to a two-step 1.19–10.71-μm frequency bridge. *Opt. Lett.* **1997**, *22*, 1211–1213. [CrossRef]
28. Sabirov, O.I.; Assanto, G.; Sapaev, U.K. Efficient Third-Harmonic Generation by Inhomogeneous Quasi-Phase-Matching in Quadratic Crystals. *Photonics* **2023**, *10*, 76. [CrossRef]
29. Norton, A.H.; de Sterke, C.M. Aperiodic 1-dimensional structures for quasi-phase matching. *Opt. Express* **2004**, *12*, 841–846. [CrossRef]
30. Sapaev, U.K.; Assanto, G. Engineered quasi-phase matching for multiple parametric generation. *Opt. Express* **2009**, *17*, 3765–3770. [CrossRef]
31. Yusupov, D.B.; Sapaev, U.K. Multistep third-harmonic generation of femtosecond laser pulses in periodically-poled and chirped-periodically-poled lithium niobate. *J. Russ. Laser Res.* **2009**, *30*, 321–326. [CrossRef]
32. Tian, Y.; Li, Q.; Yan, L.; Cao, X.; Zhao, X. A Brief Review on Nonlinear Photonic Crystals Induced by Direct Femtosecond Laser Writing. *Photonics* **2023**, *10*, 833. [CrossRef]
33. Zhu, S.; Zhu, Y.; Ming, N. Quasi-phase-matched third-harmonic generation in a quasi-periodic optical superlattice. *Science* **1997**, *278*, 843–846. [CrossRef]
34. Longhi, S. Third-harmonic generation in quasi-phase-matched $\chi^{(2)}$ media with missing second harmonic. *Opt. Lett.* **2007**, *32*, 1791–1793. [CrossRef] [PubMed]
35. Chirkin, A.S.; Volkov, V.V.; Laptev, G.D.; Morozov, E.Y. Consecutive three-wave interactions in nonlinear optics of periodically inhomogeneous media. *Quantum Electron.* **2000**, *30*, 847. [CrossRef]
36. Zhang, C.; Zhu, Y.; Yang, S.; Qin, Y.; Zhu, S.; Chen, Y.; Liu, H.; Ming, N. Crucial effects of coupling coefficients on quasi-phase-matched harmonic generation in an optical superlattice. *Opt. Lett.* **2000**, *25*, 436–438. [CrossRef]
37. Sapaev, U.; Assanto, G. On the generation of optical third-harmonic through quasi-phase-matching in quadratic nonlinear crystals. *Wave Motion* **2024**, *130*, 103372. [CrossRef]
38. Kintaka, K.; Fujimura, M.; Suhara, T.; Nishihara, H. Third harmonic generation of Nd:YAG laser light in periodically poled $LiNbO_3$ waveguide. *Electron. Lett.* **1997**, *33*, 1459–1461. [CrossRef]
39. Laurell, F.; Brown, J.B.; Bierlein, J.D. Sum-frequency generation in segmented KTP waveguides. *Appl. Phys. Lett.* **1992**, *60*, 1064–1066. [CrossRef]
40. Dmitriev, V.G.; Gurzadyan, G.G.; Nikogosyan, D.N. *Handbook of Nonlinear Optical Crystals*; Springer: Berlin/Heidelberg, Germany, 2013.

Disclaimer/Publisher's Note: The statements, opinions and data contained in all publications are solely those of the individual author(s) and contributor(s) and not of MDPI and/or the editor(s). MDPI and/or the editor(s) disclaim responsibility for any injury to people or property resulting from any ideas, methods, instructions or products referred to in the content.